PROCEEDINGS, 41st Workshop on Geothermal Reservoir Engineering
Stanford University, Stanford, California, February 22-24, 2016
SGP-TR-209

The Geochemical Response of the Rotokawa Reservoir to the First Five Years of Nga Awa Purua Production

Jeffrey A. Winick[1], Simon Addison[2], Steve Sewell[2], Etienne Buscarlet[2], Dario Hernandez[2] and Farrell Siega[2]

[1]Schlumberger Water Services, 1875 Lawrence Street, Suite 500, Denver, CO 80202

[2]Mighty River Power Limited, PO Box 245, Rotorua 3010, New Zealand

jwinick@slb.com, simon.addison@mightyriver.co.nz

Keywords: Rotokawa, geochemistry, Nga Awa Purua, dilution, silica, boiling, production

ABSTRACT

Best practice geothermal field management requires identification of the key processes acting within the reservoir, and understanding of the relationships between reservoir and process chemistry changes with the potential to impact resource and infrastructure sustainability. Following the initial development of the 34MWe Rotokawa Power Station, the Rotokawa reservoir exhibited relatively stable production geochemistry characteristics. In 2010 the 138MWe Nga Awa Purua Power Station (a joint-venture between Mighty River Power and Tauhara North No.2 Trust) was commissioned which increased steam production and brine injection in the Rotokawa reservoir. As anticipated, this generated a number of transient hydrogeologic changes which were monitored closely through regular Tracer Flow Testing (TFT), produced fluid geochemistry evaluation, in addition to a variety of other reservoir testing activities. When integrated and evaluated within a geoscientific context, these data provide important insights into both transient and long-term reservoir changes which can occur in response to operational activities. This paper will discuss the geochemical response of the Rotokawa reservoir to Nga Awa Purua start-up and operation over the last 5 years. Production well geochemistry has identified distinct geochemical responses to three main processes occurring within the reservoir: 1) injection chemical breakthrough, 2) boiling, and 3) dilution from marginal recharge.

1. INTRODUCTION

The Rotokawa geothermal field is located within the Taupo Volcanic Zone (TVZ). In 1997 the Rotokawa Power Station (RKA) was commissioned, initially as a 24 MWe Ormat combined cycle plant which was expanded to 34 MWe in 2003. In 2010 the triple-flash 138 MWe Nga Awa Purua Power Station (NAP) was commissioned.

Over the last 19 years of continuous geothermal operations at Rotokawa, the conceptual understanding of the field and reservoir geochemistry has evolved significantly. Three key reservoir processes have been identified on the basis of fluid and gas geochemistry response: 1) injection returns, 2) boiling, and 3) marginal recharge. Only through a comprehensive geochemical forensics investigation, encompassing an array of fluid and gas chemistry indicators, and integrated with other resource monitoring information, can one assess the extents to which each of these important reservoir processes may be impacting production. This paper highlights some of the geochemical changes relating to these processes and discusses their relevance to field development and operations.

A simplified configuration of production wells, injection wells, and associated power plants at the Rotokawa geothermal field is shown in Figure 1. The Rotokawa geothermal field layout is shown in Figure 2. The interconnection from the RK32-33-34 production pad enables these wells to supply either NAP or RKA. Since the interconnection of this well pad to RKA in 2013 (Hoepfinger et al., 2015), RK32 has predominantly supplied RKA, with RK33 and RK34 supplying NAP.

Three chemically distinct injection fluids are generated at the power stations on the Rotokawa geothermal field. The first is a combined condensate and brine fluid from RKA (700-720 ppm SiO_2, ~165˚C, Silica Saturation Index [SSI] ~1.0, pH_{25} ~5.1). The NAP Power Station makes use of a direct-contact condenser, and therefore the condensate (0 ppm SiO_2, ~45˚C, pH_{25} ~7) is oxygenated and is injected separately from the brine (~1150 ppm SiO_2, ~130˚C, SSI 2.3, pH_{25} 5.0). Thus NAP generates two different injection fluids. As of 2015 there are five deep wells in the southeast of the field and two intermediate aquifer wells (300-500m depth) accepting these injection fluids (Figure 2). The configuration of deep injection in 2015 is shown in Figure 1, with no NAP condensate being injected deep at that time. Therefore all deep injection wells connected to NAP are currently configured to accept brine. Since early 2011, RK21 and RK22 have not been used for injection and all NAP brine was injected into RK24, and from mid-2013 also into RK23. Prior to mid-2013, NAP condensate was injected to both shallow wells and RK23.

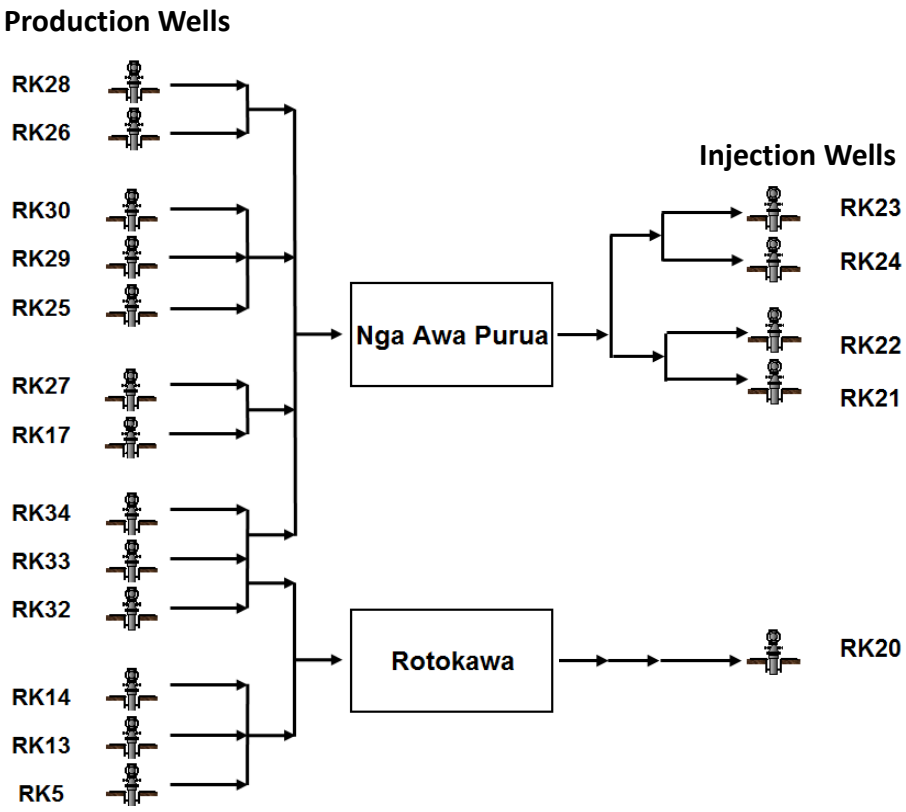

Figure 1: Simplified production well, injection well, and associated power station configuration for the Rotokawa geothermal field as of 2015.

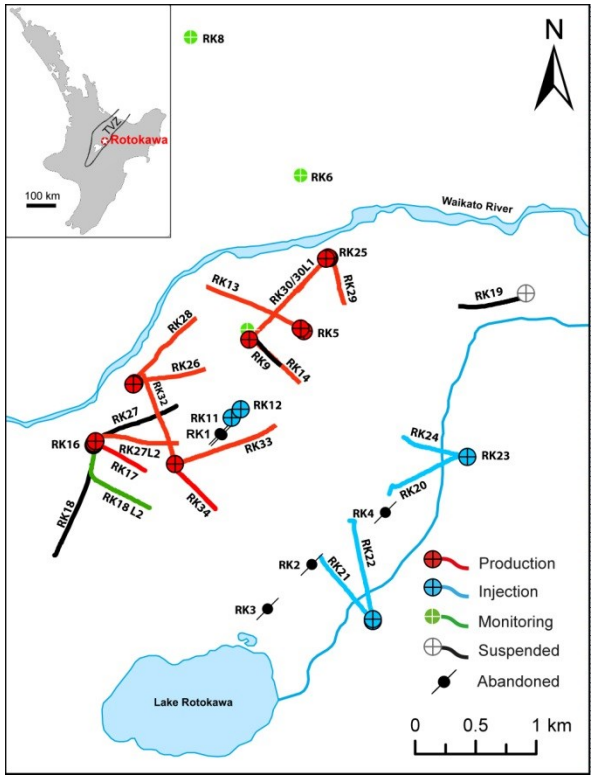

Figure 2: Rotokawa geothermal field layout as of 2015.

2. NATURAL STATE

The natural state chemistry for the Rotokawa geothermal field was first assessed by Hedenquist et al. (1988), and subsequently updated by Winick et al. (2011). Significant gradients have been documented across the field from southeast to northwest in terms of Cl, Cl/B, Na-K-Ca geothermometry and non-condensable gases (NCGs). These trends are generally perpendicular to the main NE-SW structural axis of the production field and the wider TVZ. Prior to establishment of deep injection in RK13 (December, 2004) historic discharges from wells RK4, RK5, RK6, RK9, RK13 and RK14 were representative of natural-state reservoir conditions (Figure 2).

The main geothermal upflow to the reservoir is conceptualized as a two-phase upflow in the south of the field. This rises and boils, outflowing from the system towards the north. Progressive dilution along the outflow by cooler marginal fluids, in addition to fluid-rock interactions, are thought to be responsible for the observed gradients in chemistry. However, it is noted that alternative scenarios involving multiple fluid upflows with distinct geochemical signatures have also been considered. A large structural feature in the centre of the field (referred to as the Central Field Fault) is believed to focus upflow along a zone of enhanced vertical permeability, establishing a two-phase region throughout much of the deep reservoir and the overlying intermediate aquifer (Winick et al., 2011; Sewell et al., 2015a). An intermediate aquifer overlies the deep reservoir and hosts a mixture of gas-rich steam condensates, cold groundwater, boiled reservoir fluids, and acid-SO_4-Cl fluids from a shallow, steam-heated aquifer in the vicinity of Lake Rotokawa.

3. PRODUCTION CHEMISTRY OBSERVATIONS

3.1 Sampling Program

Tracer flow testing and geochemistry sampling for both steam and brine is conducted every 2-3 months for each production well on the field. Tracer flow testing provides two-phase mass flow and enthalpy determinations. Brine and steam are sampled for geochemistry at operating well conditions. Brine geochemical analyses include: pH, conductivity, total inorganic carbon, Cl, F, SO_4, sulphide (as H_2S), As, B, Ca, Fe, Li, Mg, K, Na, NH_4, Rb, and SiO_2. The steam phase is sampled for: gas to steam ratio, and non-condensable gas (NCG) chemistry including CO_2, H_2S, CH_4, H_2, N_2, NH_3, He, O_2, and Ar.

Chemistry sampling at NAP is conducted monthly, with brine sampled after the HP, IP and LP separators. HP steam, IP steam and LP steam are sampled for NCGs as part of the emissions trading scheme reporting. Chemistry sampling at RKA is conducted approximately every two months which includes sampling of injection brine chemistry. Steam and condensate are also sampled as part of reporting requirements for the emissions trading scheme.

3.2 Sulfate

Addition of sulfuric acid (98%) to HP brine at NAP is conducted to inhibit the polymerization of silica and enable additional energy extraction during the IP and LP flash (Addison et al., 2015b). Since NAP start-up, there has been a continual decrease in the quantity of sulfuric acid required to achieve a pH_{25} set-point of 5.0 in the LP brine. This relates primarily to the loss of gas from the reservoir as described below (Section 3.4), which has resulted in reduced buffering capacity of the brine. Due to this reduction in acid addition, the concentration of sulfate in the LP brine has declined from around 130-140 ppm to ~100 ppm, as shown in Figure 3. Anomalously high sulfate measurements for RKA injection relate to sampling artefacts, whereby dissolved $H_2S_{(aq)}$ was oxidized while in sample storage prior to analysis. No increase in sulphate in the produced fluids (NAP HP brine) has been identified which might otherwise indicate recycling of injected brine. This includes production wells with confirmed injection returns on the basis of reservoir tracer tests (e.g. RK29).

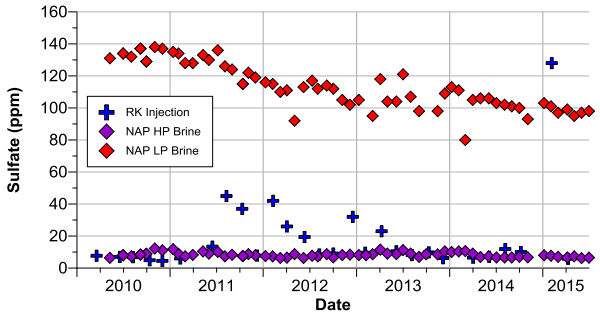

Figure 3: Sulfate results for the period 2010-present for NAP (HP brine & LP brine) and RKA injection.

Isochemical contour maps of sulfate for 2010, 2012 and 2015 are shown in Figure 7. The most notable change in sulfate relates to the slight increases observed in RK28, RK13, and RK26 following start-up of NAP. All other production wells have demonstrated stable or decreasing sulfate with time. In particular, sulfate has been stable or has slightly decreased in the southeastern production area (RK29, RK14, RK33) despite the fact that these wells are nearest to the NAP brine injection wells, and demonstrate confirmed reservoir tracers returns (Winick et al., 2015; Addison et al., 2015a). This suggests sulfate loss may occur through mineral deposition (anhydrite?) or potentially as chemical reduction of sulfate. It is noteworthy that the sulfate response in the Rotokawa geothermal reservoir is the opposite to that which is observed at Kawerau, another Mighty River Power operated plant that uses pH-modification technology. In the case of Kawerau, rising sulfate concentrations in production wells has been directly correlated with the chemical breakthrough of acidified-brine injection.

3.3 Chloride

The NAP power station contains a three-stage condensing turbine, which produces condensed steam that is processed through a cooling tower. This process results in a net evaporative loss of mass from the reservoir. As a result of this process, and assuming some level of injection recycling, total reservoir chloride concentrations are expected to increase over time. Conversely, the RKA power station is a closed circuit. Aside from a small fraction of non-condensable gas discharges, nearly 100% of the produced geothermal fluids from RKA are injected. The increases in chloride observed in the produced fluids to both power stations is associated with a combination of injection returns from NAP brine and reservoir boiling, and possibly some geochemical overprinting by dilute marginal fluid signature (Figure 4).

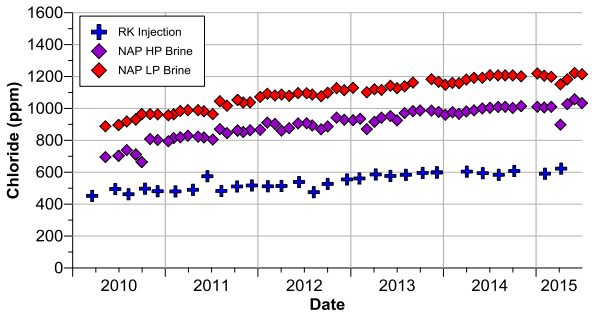

Figure 4: Chloride results for the period 2010-present for NAP (HP brine & LP brine) and RKA injection.

Marginal recharge is also likely to be providing some fluid-pressure support in the field, expressed geochemically as observed dilution in the northwest wells (RK28, RK26, and RK13). These wells also have produced slightly higher reservoir sulfate, which is unlikely to be related to injection, as no reservoir tracers have been detected in these wells. Chloride maps for 2010, 2012 and 2015 are shown in Figure 8. The observable dilution trends for the northwest wells suggests they are being recharged by a low chloride, high-sulfate marginal fluid. As a proportion of total flow to the plant, RKA receives a slightly higher mass contribution from this sector of the steamfield as compared to NAP. This is reflected in the slightly supressed chloride increases in the RKA injection brine (Figure 4).

Figure demonstrates in 2010, that approximately a 200 ppm chloride gradient was present across the main production field. By 2015 this gradient had increased to over 600 ppm, with the highest levels produced from RK17 in the southwest, and the lowest values produced from RK28. Chloride/Boron maps for 2010, 2012 and 2015 are shown in Figure 9. A Cl/B gradient across the field has been evident since natural state conditions (Hedenquist et al., 1988), however since 2010, higher Cl/B values have been observed in the southwestern wells (RK17, RK27L2), which is likely associated with boiling-induced chloride increases and boron losses.

3.4 Non-Condensable Gases

Calculated discharge quantities of CO_2 and H_2S are shown in Figure 5. Details on gas discharge monitoring are given in Lawson & Siega (2015). Upon NAP start-up in early 2010, gas discharges increased significantly for the field. With time both CO_2 and H_2S have generally declined (Figure 5).

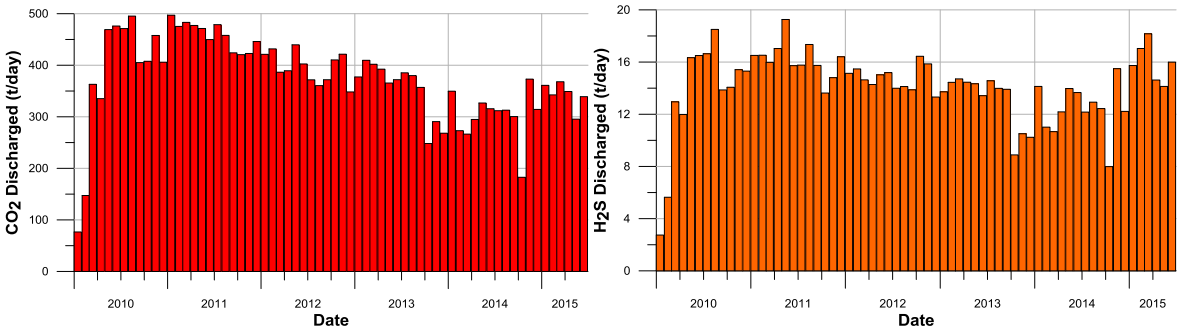

Figure 5: Calculated monthly CO_2 (left) and H_2S (right) discharges from 2010 - mid-2015 for the Rotokawa field.

Production field contours of gas in total discharge for 2010, 2012 and 2015 are shown in Figure 10. As noted in Hedenquist et al., (1988) and Winick et al., (2011), significant gradients in gas in total discharge were present across the field in the natural state condition. Since NAP start-up, low-gas has been produced by north-western wells (RK13, RK28, and RK26) and eastern wells (RK29, RK5, and RK14) which are thought to respectively reflect a source of dilute marginal recharge and chemical breakthrough from brine injection. As of 2015 a general SE-NW gradient across the field was still observable, with RK34 producing the highest values at >1.4wt% gas in total discharge.

As with gas in total discharge, CO_2/H_2S ratios of the gas discharges have also been declining, consistent with the overall reservoir pressure decline and boiling. The difference in relative solubility for CO_2 and H_2S results in the preferential loss of CO_2 from the liquid

phase, and ultimately from the Rotokawa reservoir as produced steam is processed through the power stations. As a result, reservoir brine becomes progressively enriched in H_2S relative to CO_2, resulting in declining CO_2/H_2S ratios over time.

CO_2/H_2S ratios have been contoured for the Rotokawa production field for years 2010, 2012 and 2015, are shown in Figure 11. The contour trends correlate to the general pattern of reservoir pressure-drawdown within the production field (Hernandez et al., 2015a; Sewell et al, 2015a). The western production wells (RK17, RK27, RK32), have exhibited a pronounced decline in CO_2/H_2S with increasing pressure drawdown and boiling. This topic is explored further in Section 4.2.

3.5 Silica

Increasing silica concentrations were observed in the total flow supplying NAP for two-years following plant startup and until about the beginning of 2013 (Figure 6). This trend was observed in wells that also demonstrated chloride increases as a result of reservoir boiling and/or injection returns. Also during this time, quartz geothermometry temperatures from affected wells increased to unrealistically high temperatures, suggestive of reservoir silica concentrations that may not have been in equilibrium with respect to quartz. This behavior was monitored closely due to overall concerns regarding operational silica management. However from 2013 to 2015, silica concentrations stabilized and have recently showed signs of returning to initial state concentrations.

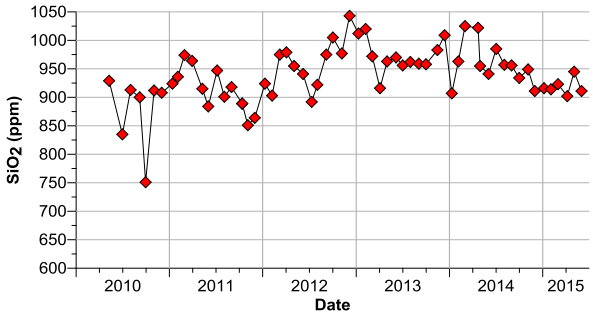

Figure 6: NAP HP brine monthly silica.

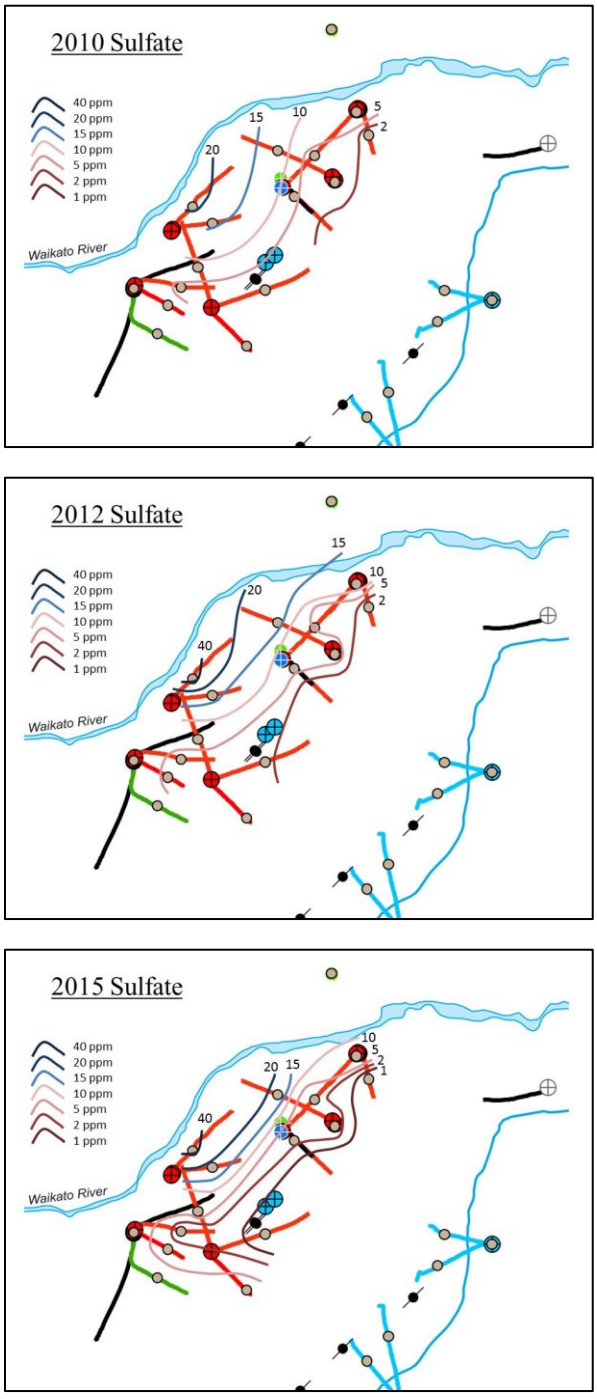

Figure 7: Reservoir sulfate for 2010, 2012 and 2015. Grey circles indicate pressure pivot points for wells where this has been identified. N.B. In 2010 RK32, RK33 and RK34 had not yet been drilled, and in 2012 RK34 had not yet been drilled. The indicated yearly average contour assessments consider only the wells available at the corresponding times.

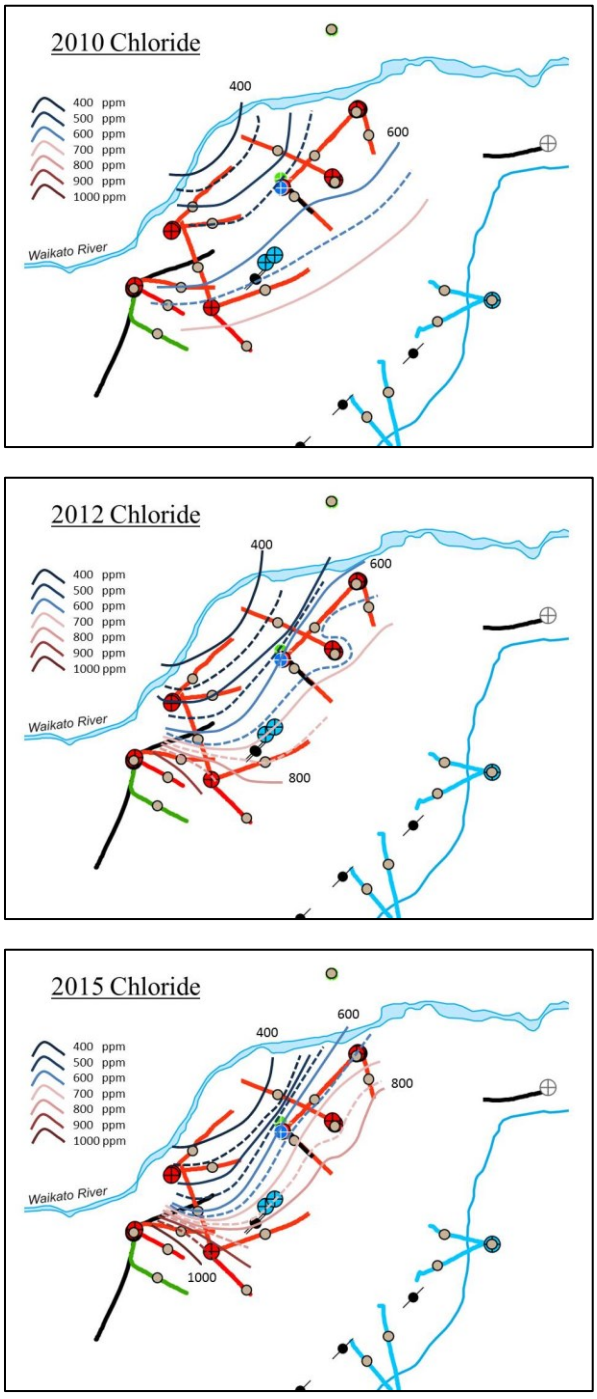

Figure 8: Reservoir chloride for 2010, 2012 and 2015. Dashed contour lines represent the 50ppm interval between each 100ppm contour.

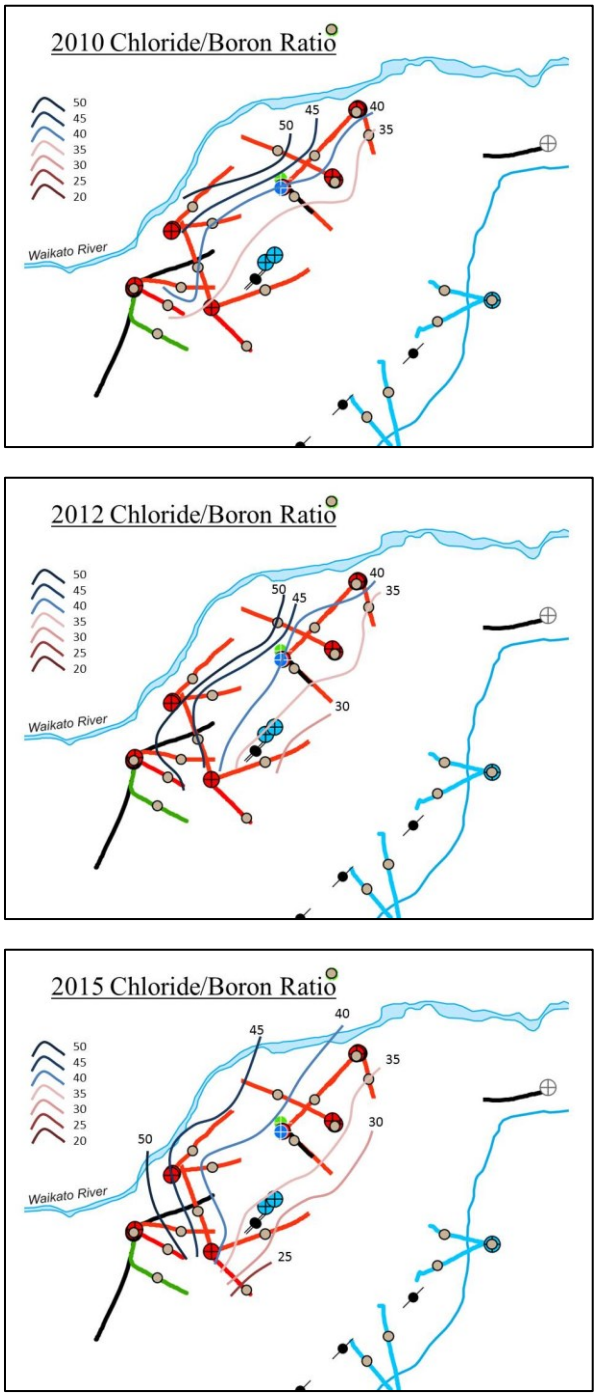

Figure 9: Reservoir chloride/boron ratios for 2010, 2012 and 2015.

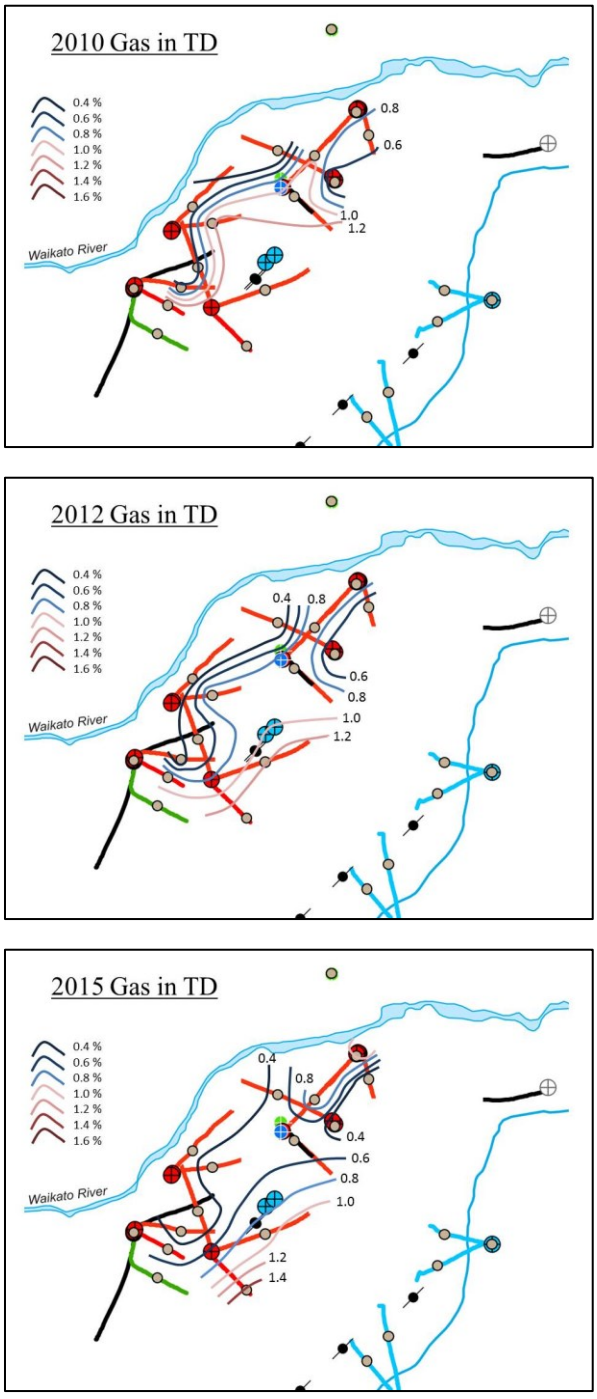

Figure 10: Gas in total discharge for 2010, 2012 and 2015.

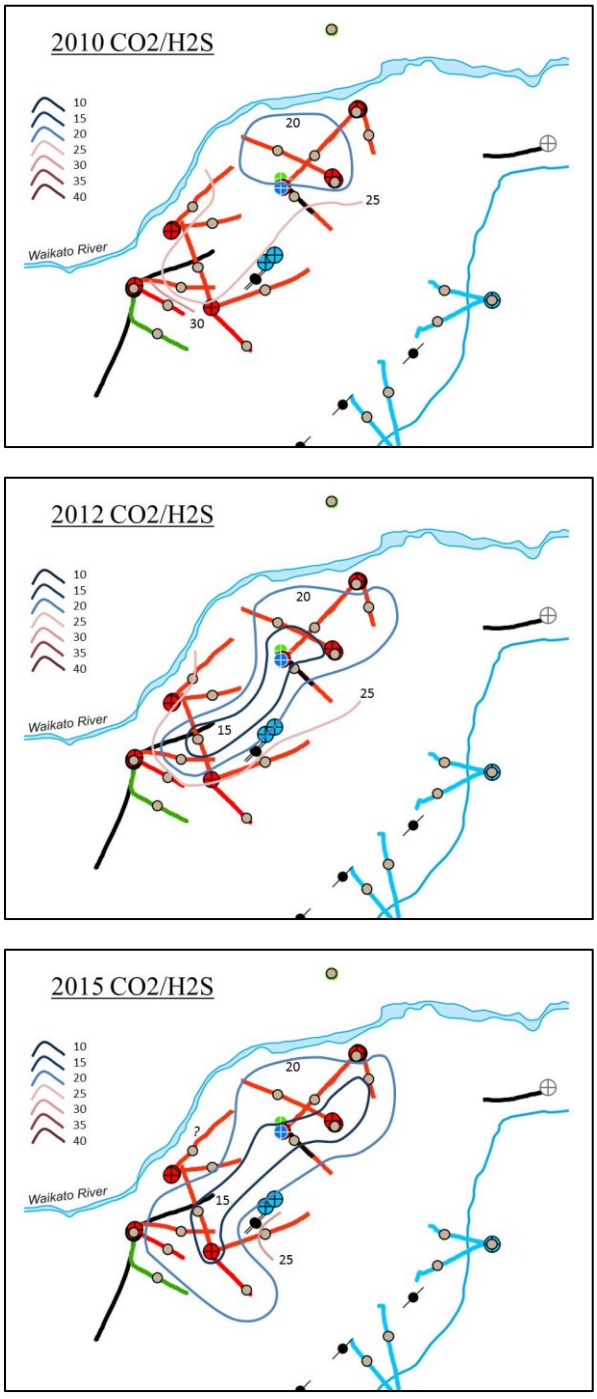

Figure 11: CO_2/H_2S ratio for 2010, 2012 and 2015.

4. OVERALL OBSERVED TRENDS

In general, the observed chemistry responses identify three different areas of the production reservoir which are variably affected by distinct reservoir processes. These reservoir areas are shown in Figure 12. The blue dashed area incorporates wells RK5, RK14, RK29 and RK33, and reflects an area demonstrating chemical breakthrough from injection. The green dashed area incorporates wells RK17 and RK27, and represents an area of significant pressure draw-down and boiling. The yellow dashed area incorporates wells RK13, RK26 and RK28, and indicates an area impacted by marginal recharge. The following sections provide additional detail regarding some of the specific geochemistry signatures and responses to the key identified reservoir processes.

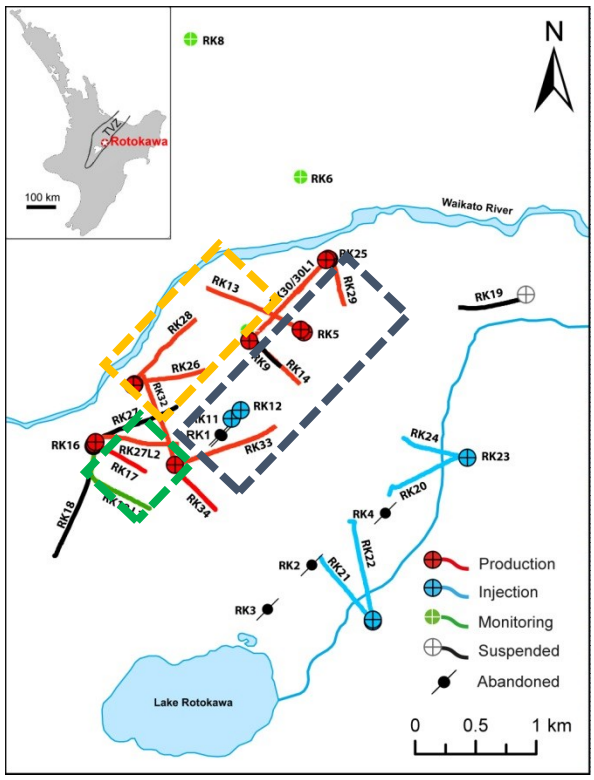

Figure 12: Map of the Rotokawa geothermal field showing key reservoir processes designated by area. Dashed blue indicates injection returns. Dashed green indicates boiling. Dashed yellow indicates marginal recharge. Each of these processes imparts distinct geochemical signatures to the produced fluids.

4.1 Injection Returns

When production from NAP was initiated, brine was injected into RK21. In late-2010, brine injection was moved to RK24. Following this change, both a chloride and pressure response was observed in wells RK5, RK14, RK29 and RK33 (Quinao et al., 2013). These wells have continued to demonstrate increasing reservoir chloride with time, as shown in Figure 13.

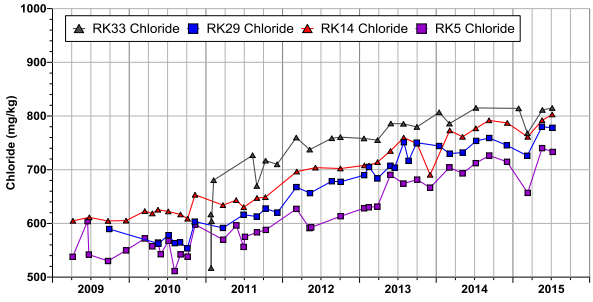

Figure 13: Chloride values for wells RK5, RK14, RK29 and RK33.

Injection returns were confirmed in these wells on the basis of the latest reservoir tracer test, conducted in 2013 (Winick et al., 2015; Addison et al., 2015a). RK29 and RK14 demonstrated the highest contributions of injection fluid contribution on the basis of the tracer test data. While RK33 has the highest level of chloride within the wells on the eastern side of the production area, on the basis of tracer test data, it demonstrates the lowest amount of injection returns amongst these wells. RK33 may be receiving fluid contributions from a high chloride source such as previous RK21 injection, or a natural state fluid up-flow inferred to exist the southern portion of the reservoir. At this point in time, gas trends for RK33 do not clearly distinguish between these possible sources.

RK29 appears to receive significant pressure support through injection from RK24. RK29 has a capacity of over 600 t/hr, and since production began from this well, it has demonstrated only a 5 bar reduction in pressure relative to natural state reservoir pressures (Hernandez et al., 2015a). The chemical evolution of RK29 is shown in Figure 14, where an increase in chloride can be observed along with an apparent decrease in sulfate, gas in steam, and gas in total discharge. An increase in quartz geothermometer temperatures is observed in RK29 which corresponds to the observed silica increases as discussed in Section 3.5 (Figure 6). Measured liquid temperatures in RK29 have remained stable between 325-330˚C over the last five years. A comparison of these temperatures to silica geothermometry indicates that 1) silica produced from RK29 might not have reached equilibrium with respect to reservoir quartz and 2)

injection derived fluid arriving to RK29 is being significantly reheated on its flow-path to the well. This reheating has also been suggested on the basis of thermal degradation of reservoir tracers (Winick et al., 2015).

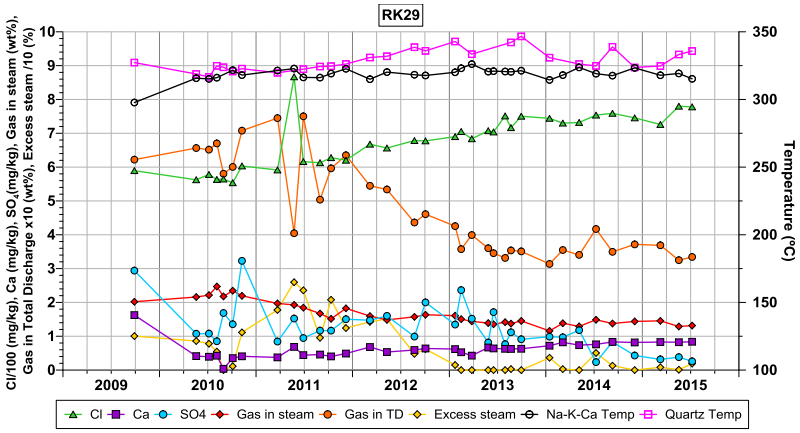

Figure 14: The evolution of key geochemistry and indicator parameters for RK29.

4.2 Boiling

RK17 and RK27L2 are part of the western pressure compartment which, on the basis of continuous pressure monitoring in RK18L2, has demonstrated ~10 bar pressure drawdown since NAP start-up (Hernandez et al., 2015a). The chloride response for RK17 and RK27L2 are shown alongside of the local reservoir pressure response in Figure 15.

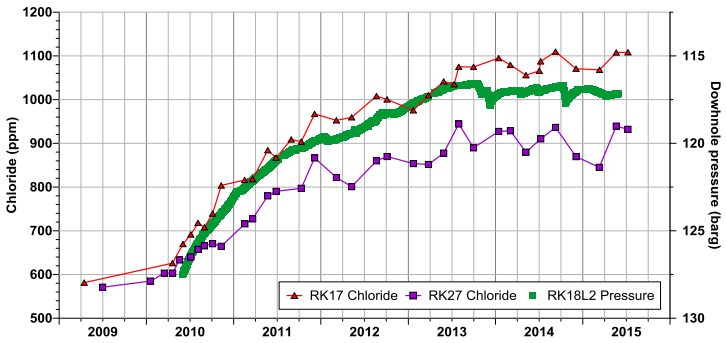

Figure 15: Chloride values for wells RK17 and RK27L2 (left axis) alongside downhole pressure measured in RK18L2 (right axis).

The western reservoir pressure compartment has demonstrated significant increases in chloride and declines in gas over time. On the basis of these observations alone, it is difficult to distinguish between a reservoir process dominated by injection fluid chemical breakthrough or by boiling, as both will generate a similar geochemical response. The lack of tracer returns in these wells and pressure declines, does suggest that boiling is the dominant process affecting this western pressure compartment.

This behavior has been investigated in more detail utilizing the relative solubility difference between CO_2/H_2S and its thermodynamically predictable response in boiling systems. The extent of boiling in this compartment was assessed through a boiling model for RK17 which incorporates known initial-state CO_2/H_2S ratios, reservoir liquid temperatures and temperature dependent vapor/liquid partitioning coefficients, and calculated reservoir steam fractions (Giggenbach, 1980). The results of the RK17 boiling model are shown in Figure 16. The modeled evolution of CO_2/H_2S ratios in response to boiling, very closely matches the observed well discharges. This strongly supports the notion that a boiling process can account for virtually all of RK17's change in output characteristics since NAP start-up.

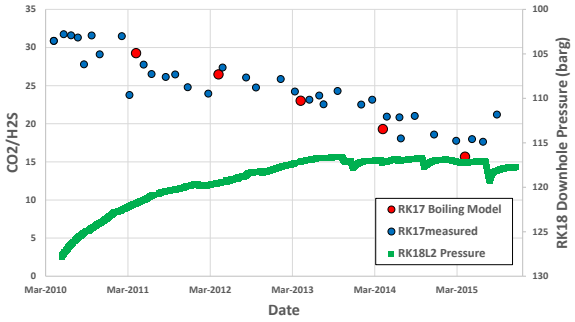

Figure 16: Modeled evolution of CO_2/H_2S in RK17 compared to observed ratios in well discharges.

4.3 Marginal Recharge

Wells RK13, RK26 and RK28 appear to be impacted by a dilute marginal fluid source. These wells demonstrate declining chloride concentrations (Figure 17) and increasing sulfate (Figure 18), consistent with contributions from a marginal fluid source to the deep reservoir. On the basis of natural state geochemistry indications (Hedenquist et al., 1988; Winick et al., 2011), a deep, dilute reservoir fluid north of the main production sector may provide this source of dilution. A similar geochemical response could be generated by ingress of intermediate aquifer fluids overlying the deep reservoir. While these wells have lower absolute geothermometer temperatures than the rest of the field, a feature also noted in the natural state condition, they have nevertheless remained stable since production start-up with no more than 5˚C measured cooling.

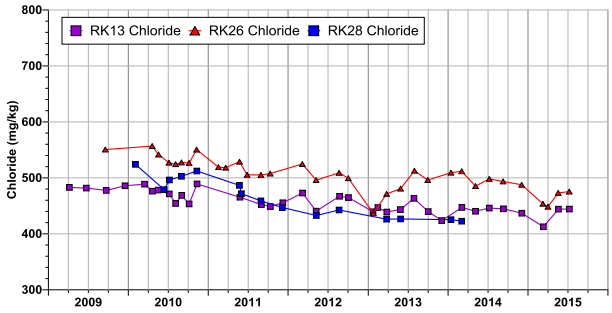

Figure 17: Chloride values for wells RK13, RK26 and RK28.

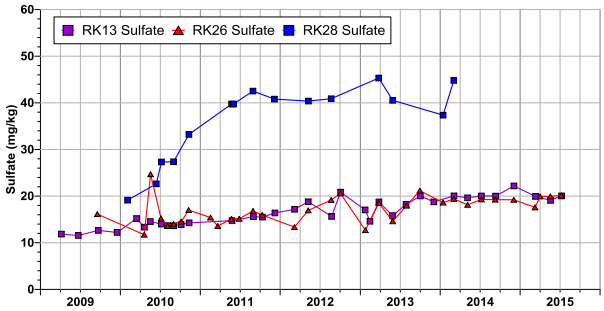

Figure 18: Sulfate values for wells RK13, RK26 and RK28.

5. CONCLUSIONS

The geochemistry of the Rotokawa reservoir has been closely monitored since the startup of Nga Awa Purua operations. A number of key geochemical indicator constituents have been evaluated and integrated with other critical resource engineering information in order to identify and monitor the behavior of important reservoir processes which impact on field sustainability. Our integrated, multi-disciplinary approach to reservoir management and monitoring has demonstrated numerous successes in operational field management at Rotokawa. We rely principally on the collection of robust geochemistry, geological, and geophysical datasets, and on the expertise of our technical resource team specialists to integrate and evaluate these datasets. Through this process Mighty River Power realizes significant value as we develop, implement, and execute field operational management plans which will ensure continued and sustainable generation at the Rotokawa geothermal field.

ACKNOWLEDGEMENTS

The authors wish to sincerely thank the Rotokawa Joint Venture (Mighty River Power and Tauhara North No.2 Trust) for permission to publish this paper. Thank you to the operations team at the Rotokawa site for their support.

Thank you to everyone involved with sampling and analysis of all samples. This includes Papawera, Western Energy Services, MB Century and GNS Science, specifically the NZ Geothermal Analytical Laboratory.

Thank you to Patrick Browne for his review of this paper.

REFERENCES

Addison, S.J., Winick, J.A., Mountain, B.W. & Siega, F.L. (2015a) Rotokawa Reservoir Tracer Test History. *Proc. NZ Geothermal Workshop.*

Addison, S.J., Brown, K.L., von Hirtz, P.H., Gallup, D.L., Winick, J.A., Siega, F.L. & Gresham, T.J. (2015b) Brine Silica Management at Mighty River Power, New Zealand. *Proc. World Geothermal Congress.*

Giggenbach, W.F. (1980) Geothermal Gas Equilibria. Geochimica et Cosmochimica Acta, Volume 44, Issue 12, p. 2021-2032

Hedenquist, J., Mroczek, E. & Giggenbach, W. (1988) Geochemistry of the Rotokawa system: Summary of data, interpretation and appraisal for energy development. Chemistry Division DSIR Technical Note. 88 (6)

Hernandez, D., Addison, S.J., Sewell, S.M., Azwar, L. & Barnes M. (2015a) Rotokawa reservoir response to 172 MW of geothermal operation. *Proc. NZ Geothermal Workshop.*

Hernandez, D., Clearwater, J., Burnell, J., Franz, P., Azwar, L. & Marsh, A. (2015b) Update on the modeling of the Rotokawa Geothermal System: 2010 – 2014. *Proc. World Geothermal Congress.*

Hoepfinger, V., Marsh, A. & Maginness, R. (2015) Adapting Surface Facilities to Changes in the Rotokawa Reservoir in the First 5 Years of Nga Awa Purua. *Proc. NZ Geothermal Workshop.*

Lawson, R. & Siega F. (2015) The Emissions Trading Scheme: Challenges and Future Impacts for Geothermal Power Plants. *Proc. NZ Geothermal Workshop.*

Quinao, J., Azwar, L., Clearwater, J., Hoepfinger, V., Le Brun, M. & Bardsley, C. (2013) Analysis and modeling of reservoir pressure changes to interpret the Rotokawa Geothermal Field response to Nga Awa Purua Power Station operation. *Proc. 38th Workshop on Geothermal Reservoir Engineering, Stanford University*

Sewell, S.M., Addison, S.J., Hernandez, D., Azwar, L. & Barnes, M.L. (2015a) Rotokawa Conceptual Model Update 5 years After Commissioning of the 138 MWe NAP Plant. *Proc. NZ Geothermal Workshop.*

Sewell, S.M., Cumming, W., Bardsley, C., Winick, J., Quinao, J., Wallis, I., Sherburn, S., Bourguignon, S. & Bannister, S. (2015b) Interpretation of microseismicity at the Rotokawa Geothermal Field, 2008 to 2012. *Proc. World Geothermal Congress*.

Winick, J., Powell, T. & Mroczek, E. (2011) The Natural-State Geochemistry of the Rotokawa Reservoir. *Proc. NZ Geothermal Workshop*

Winick, J.A., Siega, F.L., Addison, S.J., Richardson, I.M., Mountain, B.W. and Barry, B.J. (2015) Coupled Iodine-125 and 2NSA Reservoir Tracer Testing at the Rotokawa Geothermal Field, New Zealand. *Proc. World Geothermal Congress*